RSC Advances

ROYAL SOCIETY OF CHEMISTRY

www.rsc.org/advances

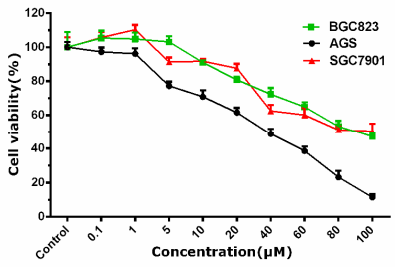

A new ruthenium complex(**Ru-adpa)** characterized by single X-ray diffraction exhibits excellent cytoxtocity against AGS cells.

Synthesis, Characterization, Crystal structure, Cytotoxicity, Apoptosis and Cell Cycle Arrest of Ruthenium(Ⅱ) Complex $[Ru(bpy)_2(adpa)](PF_6)_2$(bpy=2,2′-bipyridine, adpa = 4-(4-aminophenyl)diazenyl-N-(pyridin-2-ylmethylene)aniline)

Yan Zhang [a], Peng-Chao Hu [b], Ping Cai*[a], Fang Yang *[c], Gong-Zhen Cheng*[a]

[a] College of Chemistry and Molecular Sciences, Wuhan University, Wuhan, China, 430072

[b] Department of Pathology and Pathophysiology, Hubei Provincial Key Laboratory of Developmentally Originated Disease, School of Medicine, Wuhan University, Wuhan, China, 430072

[c] Department of Physiology, School of Medicine, Wuhan University, Wuhan, China, 430072

Abstract: A novel ruthenium(Ⅱ) complex $[Ru(bpy)_2(adpa)](PF_6)_2$(bpy=2,2′-bipyridine, adpa = 4-(4-aminophenyl)diazenyl-N-(pyridin-2-ylmethylene)aniline) (**Ru-adpa**) was synthesized, characterized and confirmed by X-ray diffraction studies. The cytotoxic potential of the complex was tested on AGS、BGC823 and SGC7901 cancer cells, the viability of the treated cells was evaluated by MTT assay and colony formation assay. The mode of cell death was assessed by different morphological study of DNA damage and apoptosis assays (Hoechst staining, Acridine orange & ethidium bromide (AO & EB) staining and flow cytometry assay). The **Ru-adpa** induced cell death in a dose- and time-dependent manner, and the mode of cell death was essentially apoptosis though necrosis was also noticed. Cell cycle analysis by flow cytometry indicated that the **Ru-adpa** caused cell cycle arrest and accumulated cells in S phase. The DNA binding properties with **Ru-adpa** was studied by gel electrophoresis.

Keywords: Ru(Ⅱ) complex; Cytotoxicity; Cell apoptosis; Cell cycle arrest

1. Introduction

Development of more efficient anticancer drugs with better selectivity but less toxic

side effects is currently an area of intense research in bioinorganic chemistry.[1-2] Since the two ruthenium complexes, NAMI-A and KP1019 entered clinical trials, more and more attention have been paid to the ruthenium complexes as potential anticancer drugs. [2-7] Recently, many Ru(Ⅱ) complexes were reported to exhibit high anticancer activity in vitro and in vivo.[8-16] For example, the field of antitumoural and antimetastatic arene ruthenium complexes pioneered by Dyson and Sadler, Ru(η^6-*p*-cymene)Cl_2(pta) (pta=1,3,5-triaza-7-phospha-tricyclo-[3.3.1.1]decane) and [(η^6-C_6H_5Ph)Ru(*N*,*N*-en)Cl]$^+$ (en = 1,2-ethylenediamine), exhibited high activity to lung metastases in mice.[18-19] The Ru(Ⅱ) polypyridyl complexes [Ru(dip)$_2$(1-Py-βC)]$^{2+}$(dip is 2,2′-bipyridine or 1,10-phenanthroline, 1-Py-βC is 1-(2-pyridyl)-b-carboline) exhibited very high cytotoxicity toward Hela cells.[20] [Ru(bpy)$_2$(dppz)]$^{2+}$(bpy is 2,2′-bipyridine, dppz is dipyrido[3,2-a;2′,3′-c]phenazine) exhibited moderate anticancer activity against HT-29 cells (IC_{50} = 26.9μM).[21]

On the other hand, Schiff bases have regularly been studied as ligands in coordination chemistry as a result of their good metal binding ability. The bidentate and multidentate Schiff bases with delocalized π-orbitals are suitable ligands for the metals of biological importance, and the study of the chemical properties of such metal-Schiff base complexes also represents a good strategy for the design and synthesis of models of biological systems.[22-25] For example, the Ru(Ⅱ) complex Ru(Ⅱ)-2,6-bis(2,6-diisopropylphenyliminomethyl)pyridine exhibits very high cytotoxicity toward cancer cells,[26] and Ru(Ⅱ)-bis(arylimino)pyridine complexes with the co-ligands 1,10-phenanthroline(phen), 2,2′-dipyridyl(bpy) can effectively inhibit the proliferation of the cancer cell lines with a low half-maximal inhibitory concentration (IC_{50}).[27] These studies stimulate us to combine Ru metal with Schiff base to study it's cytotoxicity toward cancer cells. So in this work, a new **Ru-adpa**, [Ru(bpy)$_2$(adpa)](PF_6)$_2$(bpy=2,2′-bipyridine,adpa=4-(4-aminophenyl)diazenyl-N-(pyridin-2-ylmethylene)aniline) was synthesized and characterized by elemental analysis, electrospray ionization mass spectrometry (ESI-MS), ^{1}H NMR spectroscopy and X-ray diffraction. Its cytotoxicity in vitro was evaluated by MTT (3-(4,5-dimethylthiazol-2-yl)-2,5-diphenyltetrazolium bromide) assay. The

morphological apoptosis and the percentage of necrotic and apoptotic AGS (human gastric carcinoma) cells induced by **Ru-adpa** were also studied by fluorescence microscopy and flow cytometry. The cell cycle distribution of AGS cells was investigated by flow cytometry. The DNA binding properties with **Ru-adpa** was studied by gel electrophoresis.

2. Experimental

2.1 Materials and instrumentation

All reagents and solvents were of commercial origin and were used without further purification unless otherwise noted. Ultrapure Milli-Q water was used in all experiments. Dimethyl sulfoxide (DMSO) and RPMI 1640 were purchased from Sigma. AGS (human gastric carcinoma), BGC823 (human gastric carcinoma), and SGC-7901 (human gastric carcinoma) cell lines were purchased from the American Type Culture Collection. $RuCl_3 \cdot 3H_2O$ was purchased from the Chang Cheng shiji, 4,4′-diaminoazobenzene[28] and $Ru(bpy)_2.2H_2O$[29] were prepared by published methods. Microanalysis (C, H, and N) was conducted with a PerkinElmer 240Q elemental analyzer. Electrospray ionization mass spectra(ESI-MS) were recorded with an LCQ system(Finnigan MAT, USA) using CH_3OH as the mobile phase. 300 MHz ^1H NMR spectroscopic measurements were performed on a Bruker AM-300 NMR spectrometer, using d_6-DMSO as solvent and TMS ($SiMe_4$) as an internal reference at 25°C. Infrared spectra were recorded on a Perkin-Elmer Spectrum FT-IR spectrometer using KBr pellets. UV-*vis* spectra were obtained at room temperature on Shimmadzu 3100 spectrophotometer in DMSO.

2.2 Synthesis

2.2.1 Synthesis of adpa

The ligand adpa was synthesised according to its analogues.[30] Yield: 75%. Anal. Calcd (%) for $C_{18}H_{15}N_5$: C, 71.76; H, 4.98; N, 23.25. Found (%): C, 71.80; H, 4.94; N, 23.26. ^1H NMR (300 MHz, $CDCl_3$, TMS) [ppm]: δ = 6.27 (s, 2H, $-NH_2$), 7.40 (d, 2H, Ph, J = 9.0 Hz), 7.47(m, 1H, Py), 7.50(m, 1H, Py), 7.55 (m, 1H, Ph), 7.84 (m, 2H, Ph), 7.92 (d, 2H, Ph, J = 6.0 Hz), 7.99 (d, 2H, Ph, J = 9.0 Hz), 8.22 (d, 1H, Py), 8.66 (s, 1H, -CH=N), 8.74 (d, 1H, Py). IR (KBr) [cm^{-1}]: 3308(ν_{N-H}), 1626, 1586, 1464, 1349

($\nu_{C=C}$, $\nu_{C=N,}$ $\nu_{N=N}$), 856, 740(δ_{C-H}).

2.2.2 Synthesis of the $[Ru(bpy)_2(adpa)](PF_6)_2$ (Ru-adpa)

An ethanol solution of $AgNO_3$ (0.17 g, 1.0 mmol) was added to an ethanol solution of $[Ru(bpy)_2Cl_2]\cdot 2H_2O$ (0.26 g, 0.5 mmol). After refluxing for 30 min and filtering to remove the deposited AgCl, the ligand adpa (0.15 g, 0.5 mmol) was added, the solution was refluxed for 12 h under N_2, and then evaporated to 5 mL, on cooling, a red precipitate was obtained by dropwise addition of saturated aqueous KPF_6, then filtered, the filtrate was placed and evaporated, two weeks later, $[Ru(bpy)_2(adpa)](PF_6)_2$ was obtained as a red crystal. Yield: 70 %. Anal. Calcd (%) for $C_{38}H_{31}N_9P_2F_{12}Ru$: C, 45.42; H, 3.09; N, 12.55. Found(%): C, 45.43; H, 3.09; N, 12.59. ^{1}H NMR (300 MHz, d_6-DMSO, TMS) [ppm]: δ=6.29 (s, 2H, -NH_2), 6.66 (d, 2H, Ph, J = 7.5 Hz), 7.41 (d, 4H, bpy, J = 9.0 Hz), 7.51(m, 1H, Py), 7.62(m, 1H, Py), 7.76(m, 4H, bpy), 7.84 (m, 2H, Ph), 7.90 (d, 2H, Ph, J = 6.0 Hz), 7.99 (d, 2H, Ph, J = 9.0 Hz), 8.21 (d, 4H, bpy), 8.22 (d, 1H, Py), 8.62 (s, 1H, -CH=N), 8.75 (d, 1H, Py), 8.85 (d, 4H, bpy). IR (KBr) [cm^{-1}]: 3388(ν_{N-H}), 1591, 1515, 1381, 1129 ($\nu_{C=C}$, $\nu_{C=N,}$ $\nu_{N=N}$), 835, 759(δ_{C-H}). ESI-MS: m/z 860.0 for ($[M-PF_6]^+$), 357.6 for $[M-2PF_6]^{2+}$. UV-*vis* (DMSO, $\lambda_{max}/\varepsilon$)[$nm/dm^3\cdot mol^{-1}\cdot cm^{-1}$]: 292($6.90\times10^4$), 460($2.02\times10^4$).

2.3 Methods

2.3.1 Single crystal X-ray structure determinations

The X-ray diffraction experiments were carried out with a Bruker Apex Ⅱ CCD area detector diffractometer, using graphite-monochromated Mo-Kα radiation (λ= 0.71073 Å) at 100(2) K. Absorption corrections were applied semi-empirically using the APEX2 program.[31] The structures were solved by direct methods and refined by the full-matrix least-squares against F^2 in an anisotropic (for non-hydrogen atoms) approximation. All calculations were performed using the SHELXTL software.[32]

2.3.2 Cytotoxicity assay in vitro

Standard MTT assay procedures were used.[33] Cells were placed in 96-well microassay culture plates (8×10^3 cells per well) and grown overnight at 37 °C in a 5% CO_2 incubator. The complex tested was then added to the wells to achieve final concentrations ranging from 10^{-7} to 10^{-4} M. Control wells were prepared by addition

of culture medium (200 μL). The plates were incubated at 37 °C in a 5% CO_2 incubator for 48 h. On completion of the incubation, stock MTT dye solution (20 μL, 5 mg/mL) was added to each well. After 4 h, 150 mL dimethylsulfoxide (DMSO) was added to solubilize the MTT formazan. The optical density of each well was then measured with a microplate spectrophotometer at a wavelength of 490 nm. The IC_{50} values were determined by plotting the percentage viability versus the concentration and reading off the concentration at which 50% of the cells remained viable relative to the control. Each experiment was repeated at least three times to obtain the mean values. Three different tumor cell lines were the subjects of this study: AGS, BGC823 and SGC-7901. These cells were purchased from the American Type Culture Collection (Rockville, MD, USA).

2.3.3 Colony formation assay

The cells were plated in six-well plates at 2000 cells per well. 24 h later, the complex was added to the plates. After treatment, fresh medium was applied to the plates. The cells were allowed to grow for ten additional days before staining with Crystal Violet (Sigma). All experiments were repeated at least three times, and similar results were obtained in each trial.

2.3.4 Apoptosis assay by acridine orange (AO) and ethidium bromide (EB) staining[34]

AGS cells were seeded in 6-well plates and allowed to reach 70% confluence. The cells were then treated with different concentrations of the complex for 24 or 48 h. The cells were trypsinized and pelleted, and then suspended in PBS. A drop of cell suspension was placed on a glass slide and stained with AO & EB and a cover slip was laid over to reduce light diffraction. At random 300 cells were observed in a fluorescent microscope(Nikon, Yokohama, Japan) fitted with a 377-355 nm filter, and observed at x400 magnification.

2.3.5 Apoptosis assay by Hoechst 33258 staining

AGS cells were seeded onto chamber slides in six-well plates at a density of 2×10^5 cells per well and incubated for 24 h. The cells were cultured in RPMI 1640 supplemented with 10 % fetal bovine serum (FBS) and incubated at 37 °C and 5%

CO_2. The medium was removed and replaced with medium (final DMSO concentration, 0.05% v/v) containing the complex for 24 or 48 h. The medium was removed, and the cells were washed with ice-cold phosphate-buffered saline(PBS), and fixed with formalin (4%, w/v). Cell nuclei were counterstained with Hoechst 33258 (10 mg/mL in PBS) for 10 min. Then the cells were observed and imaged by a fluorescence microscope (Nikon, Yokohama, Japan) with excitation at 350 nm and emission at 460 nm.

2.3.6 Apoptosis assay by flow cytometry

After chemical treatment, 2×10^5 cells were harvested, washed with PBS, then fixed with 70% ethanol, and finally, maintained at 4 °C for at least 12 h. Then the pellets were stained with the fluorescent probe solution containing 50 μg/mL propidium iodide and 1 mg/mL annexin in PBS on ice in the dark for 15 min. The fluorescence was then measured at 530 and 575 nm using 488-nm excitation by a FACSCalibur flow cytometry system. A minimum of 10,000 cells were analyzed per sample.

2.3.7 Cell cycle arrest investigated by flow cytometry

AGS cells were seeded into six-well plates at a density of 2×10^5 cells per well and incubated for 24 h. The cells were cultured in RPMI 1640 supplemented with FBS(10%) and were incubated at 37 °C and 5% CO_2. The medium was removed and replaced with medium (final DMSO concentration, 0.05 % v/v) containing complex. After incubation for 24 h, the cell layer was trypsinized and washed with cold PBS and fixed with 70 % ethanol. 20 μL of RNase (0.2 mg/mL) and 20 μL of propidium iodide (0.02 mg/mL) were added to the cell suspensions and they were incubated at 37 °C for 30 min. Then the samples were analyzed with a FACSCalibur flow cytometry system. The number of cells analyzed for each sample was 10,000.

2.3.8 Gel electrophoresis

The lpBR322 (linear pBR322) was obtained by the cleavage of pBR322 with Bam HI (New England Biolabs, USA). The mixing ratios of complex/EB/H33258 and pBR322 base pairs were 0, 1:1, 2:1 and 4:1. Electrophoresis was conducted at 120 V for 30-40 min in a Tris/borate/EDTA buffer solution using 1% agarose gels to analyze DNA. The gel was stained with EB and photographed using UV illumination.

3. Results and discussion

3.1 Synthesis and characterization

Schiff base ligand (adpa) was synthesized by 4,4′-diaminoazobenzene and 2-pyridine formaldehyde in ethanol. **Ru-adpa** was prepared by direct reaction of adpa with appropriate precursor complex relatively high yield (Scheme 1). The desired **Ru-adpa** was isolated as the hexafluorosphate and purified by recrystallization. ESI-MS spectra of the **Ru-adpa** exhibited two strong peaks at 357.6 and 860.0, which were assigned to $[Ru(bpy)_2(adpa)]^{2+}$ and $[Ru(bpy)_2(adpa)\cdot PF_6]^+$, respectively (The IR、^{1}H NMR and ESI-MS of the **Ru-adpa** in Supporting Information Fig.S1). The observed peaks revealed that the synthetic complex was Ru(Ⅱ) center and stable in the solution.

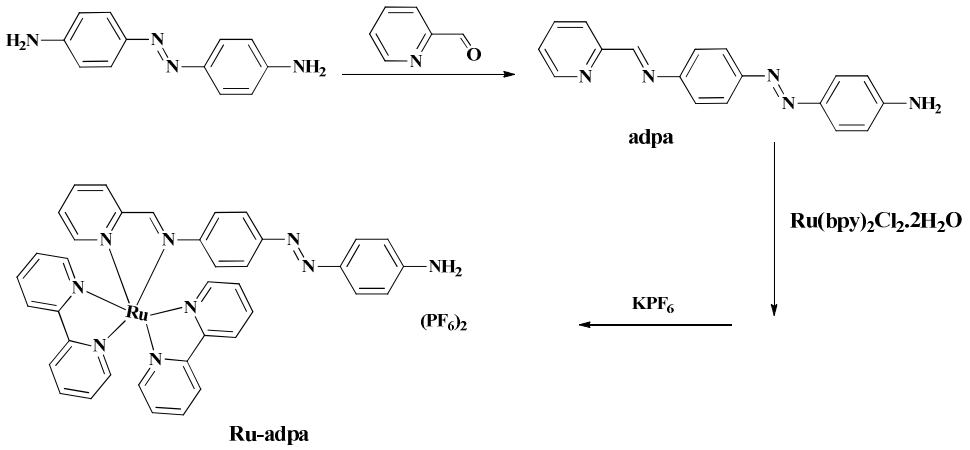

Scheme 1 Synthetic route of the adpa and **Ru-adpa**

The molecular structure of **Ru-adpa** was further confirmed by single crystal X-ray diffraction analysis. The single crystal of **Ru-adpa** was obtained from ethanol solvent by evaporating. The crystal data and refinement details for **Ru-adpa** are in Table 1. The ORTEP drawings of **Ru-adpa** with atomic numbering scheme are depicted in Fig. 1. It can be seen that the coordination sphere around the ruthenium centre constitutes a distorted octahedron with coordination of the bidentate(N-N) ligand adpa and two 2,2′-bipyridine molecules. The Ru-N bond distance for the two bpy ligands are between 2.056 and 2.070 Å, which are shorter than those with the adpa moiety (Ru1-N1 2.072(6) and Ru1-N2 2.072(5) Å, respectively) because of the greater π back-bonding into the bpy moiety to stabilize the additional electron density on the metal center donated by bpy.

Table 1 Crystal data for **Ru-adpa**

	Ru-adpa
Molecular formular	$C_{38}H_{31}F_{12}N_9P_2Ru$
Mr	1004.860
Crystal system	Triclinic
Space group	P-1
a(Å)	10.430(2)
b(Å)	11.600(2)
c(Å)	19.635(4)
α(°)	89.474(3)
β(°)	84.908(4)
γ(°)	83.509(3)
V(Å^3)	2351.1(8)
Z	2
T(K)	298(2)
D_c(g/cm^3)	1.54932
M(mm^{-1})	0.496
No. refs measured	8166
No. unique refs	764
R_1	0.0729
wR_2	0.1773
Goofs	1.034

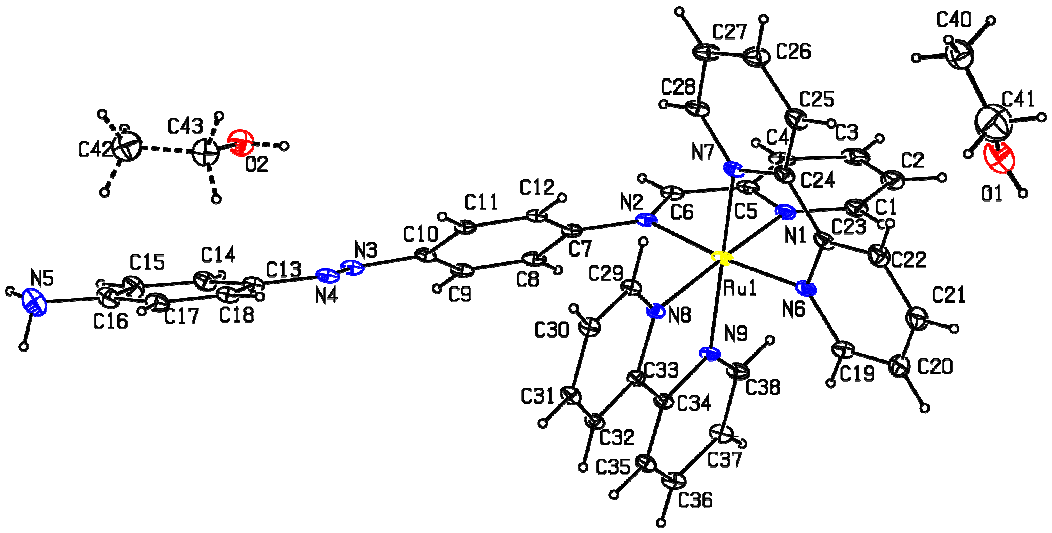

Fig. 1 ORTEP view of the molecule of **Ru-adpa** with atom-labeling scheme and thermal ellipsoids drawn at 50% probability level. Selected bond distances (Å) and angles (°): Ru1–N1 2.072(6), Ru1–N2 2.072(5), Ru1–N6 2.063(6), Ru1–N7 2.056(5), Ru1–N8 2.064(5), Ru1–N9 2.070(5), N7–Ru1–N6 78.6(2), N7–Ru1–N8 95.1(2), N6–Ru1–N8, 87.5(2), N7–Ru1–N9 173.3(2), N6–Ru1–N9, 97.5(2), N8–Ru1–N9, 79.2(2), N7–Ru1–N1 90.8(2), N6–Ru1–N1 95.8(2), N8–Ru1–N1 173.7(2), N9–Ru1–N1 95.0(2), N7–Ru1–N2 99.5(2), N6–Ru1–N2 173.9(2), N8–Ru1–N2 98.5(2), N9–Ru1–N2 85.0(2), N1–Ru1–N2 78.4(2).

3.2 Cytotoxicity assay in vitro

The cytotoxicity of the **Ru-adpa** was studied in AGS, BGC823 and SGC7901 cell lines by means of the MTT cell survival assay. AGS, BGC823 and SGC7901 cells were treated with different concentrations of **Ru-adpa** for 24、48、72、96 and 120 h. For 48 h (Fig.2a), the complex showed the highest activity in the AGS cell lines with IC_{50} values of 27.92 μM, and was moderate with IC_{50} values of 91.84 for BGC823 and 87.78 for SGC7901, respectively. For 72 h (Fig.2b-2d), the IC_{50} of the complex was 11.09 μM for AGS, 23.32 μM for BGC823 and 38.75 μM for SGC-7901. The IC_{50} of **Ru-adpa** to AGS, BGC823 and SGC7901 in different time was displayed in Table 2. Obviously, the cell viability was found to be concentration-dependent and duration-dependent, which indicated that the **Ru-adpa** entered the cells slowly and killed the cells gradually. The colony formation assay was performed to examine the effect of **Ru-adpa** on AGS growth. As shown in Fig.3, AGS cells generated fewer

colonies with increasing of **Ru-adpa** concentration, suggesting that colony was concentration-dependent. Treated with 5μM of complex, the colony number was about three times as much as 10μM, treated with 20μM of complex, the colony number was nearly zero.[35]

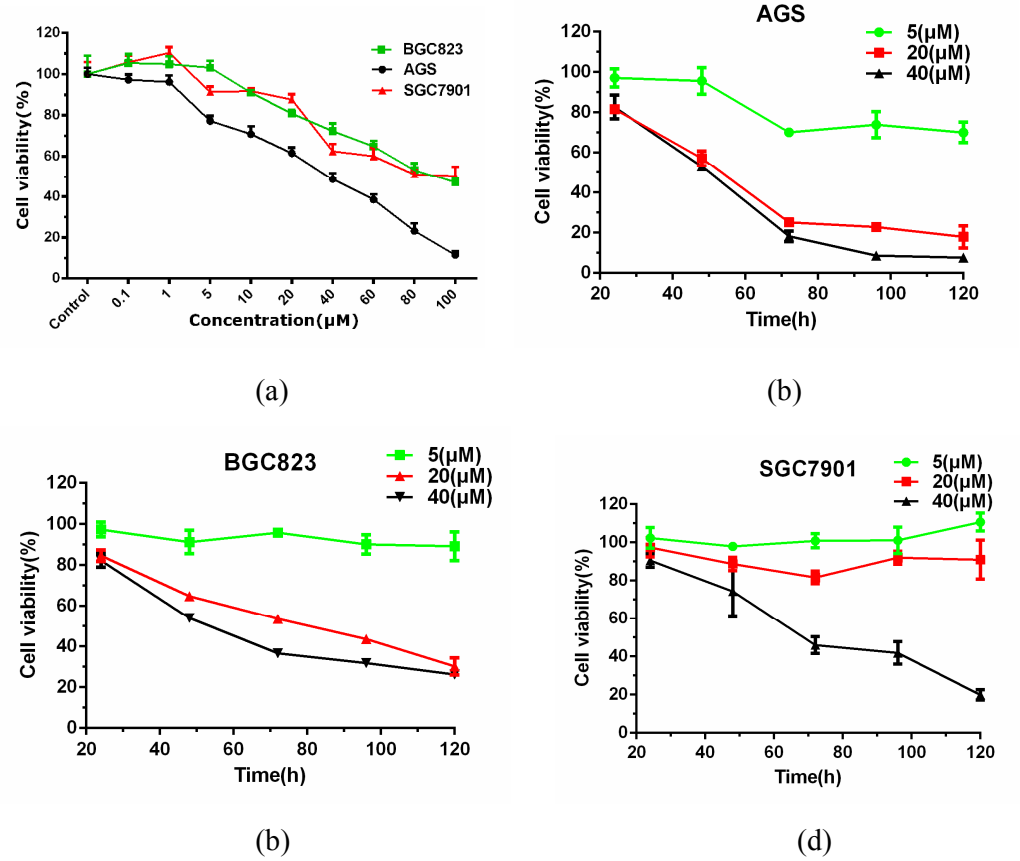

Fig. 2 (a) Cell viability of **Ru-adpa** toward proliferation of AGS, BGC823 and SGC7901 in 48 h, (b) (c) (d) Time gradient of **Ru-adpa** to AGS, BGC823 and SGC-7901

Table 1 The IC_{50} of **Ru-adpa** to AGS, BGC823 and SGC-7901 in different time

Ru-adpa	IC_{50}(μM)		
	AGS	BGC823	SGC-7901
24	>100	>100	>100
48	27.92	91.84	87.78
72	9.82	25.01	37.37
96	9.53	19.43	36.87
120	8.33	14.74	30.83

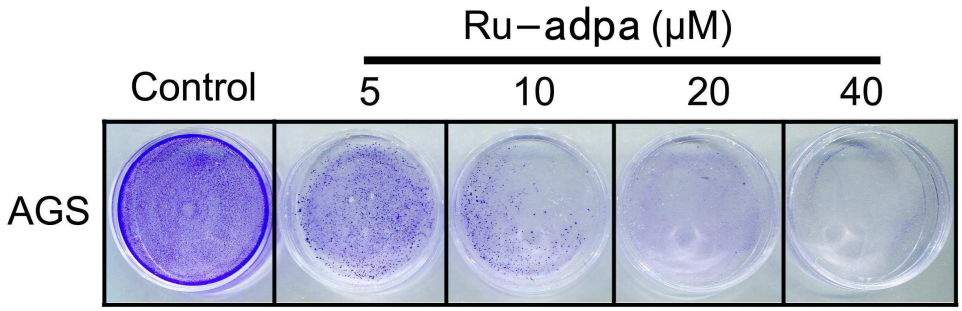

Fig. 3 Antineoplastic activity of **Ru-adpa** by colony formation assay.

3.3 Apoptosis studies by acridine orange and ethidium bromide (AO & EB) staining

AO & EB staining followed by fluorescent microscopy revealed apoptosis from the perspective of fluorescence emission. The cells were classified into four types according to the fluorescence emission and the morphological features of chromatin condensation in the nuclei: (1) The viable cells had uniformly green fluorescing nuclei with a highly organized structure. (2) Early apoptotic cells (which possessed intact membrane but DNA fragmentation was initiated) had green fluorescing nuclei, but peri-nuclear chromatin condensation was visible as bright green patches or fragments. (3)Late apoptotic cells had orange to red fluorescing nuclei with condensed or fragmented chromatin. (4)Necrotic cells had uniformly orange to red fluorescing nuclei with no indication of chromatin fragmentation, and the cells were swollen.[36] Representative images of the cells treated with **Ru-adpa** are shown in Fig. 4. The AGS cells treated with **Ru-adpa** exhibited higher incidence of apoptosis than necrosis. In the 48 h treatment group the percentage of apoptotic cells was higher than 24 h, which means that the incidence of apoptosis increased in duration-dependent manner.

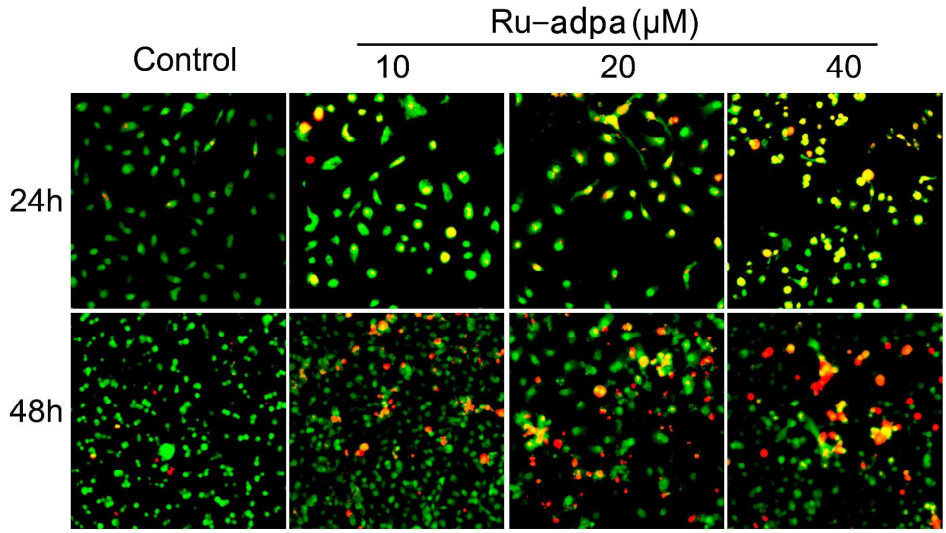

Fig.4 Photographs showing the feature of AO/EB stained AGS cancer cells

3.4 Apoptosis studies by Hoechst 33258 staining and flow cytometry

Hoechst 33258, which stains the cell nucleus, is a membrane permeable dye with blue fluorescence. Live cells with uniformly light blue nuclei were observed under fluorescence microscope after treatment with Hoechst 33258, while apoptotic cells had bright blue nuclei on account of karyopyknosis and chromatin condensation, whereas, the nuclei of dead cells could not be stained.[37] AGS cells dealt with **Ru-adpa** at 10、20 and 40 μM from 24 to 48 h were stained with Hoechst 33258. AGS cells without dealing with the **Ru-adpa** was used as control. The results were given in Fig. 5. In the control, cells show homogeneous nuclear staining. After treatment of AGS cells with **Ru-adpa**, the number of apoptotic cells increases in a dose-dependent and time-dependent manner and they exhibit typical apoptotic features, such as staining brightly, condensed chromatin, and fragmented nuclei. These results show the **Ru-adpa** can effectively induce the apoptosis against AGS cells.

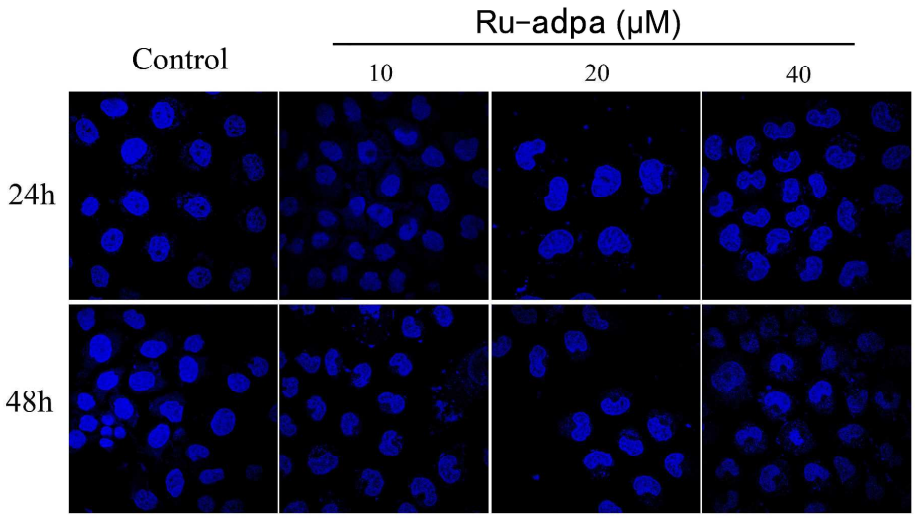

Fig.5 Hoechst 33258 staining of AGS cells

The morphological apoptosis studies showed **Ru-adpa** can induce apoptosis of AGS cells. To determine the percentages of apoptotic and necrotic cells, AGS cells without dealing with the **Ru-adpa** was used as control, apoptosis was investigated by flow cytometry, as shown in Fig.6. In the control, the proportions of living cells and apoptotic cells were 93.1 and 2.2 %, respectively. After AGS cells have been exposed to **Ru-adpa** (5、10、20、40 μM) for 12 h, the proportions of apoptotic cells were 7.8, 14.4, 14.5 and 36.1%, respectively. Comparing with the control, the proportion of living cells decreased and apoptotic cells increased. For treatment of AGS cells with **Ru-adpa** (5、10、20、40 μM) for 24 h, the proportions of apoptotic cells were 12.6, 18.8, 22.4 and 45.3%, respectively. For treatment of AGS cells with **Ru-adpa** (5、10、20、40μM) for 48 h, the proportions of apoptotic cells were 16.9, 38.8, 41.7 and 9.9%, respectively. These data demonstrate that the apoptotic effect on AGS cells for **Ru-adpa** is concentration-dependent, with increasing concentrations of **Ru-adpa**, the number of apoptotic cells increases. In addition, the apoptotic effect on AGS cells for **Ru-adpa** is duration-dependent, as time go on, the number of apoptotic cells increases. However, after AGS cells have been exposed to 40μM **Ru-adpa** for 48 h, the proportions of necrotic cells increased.

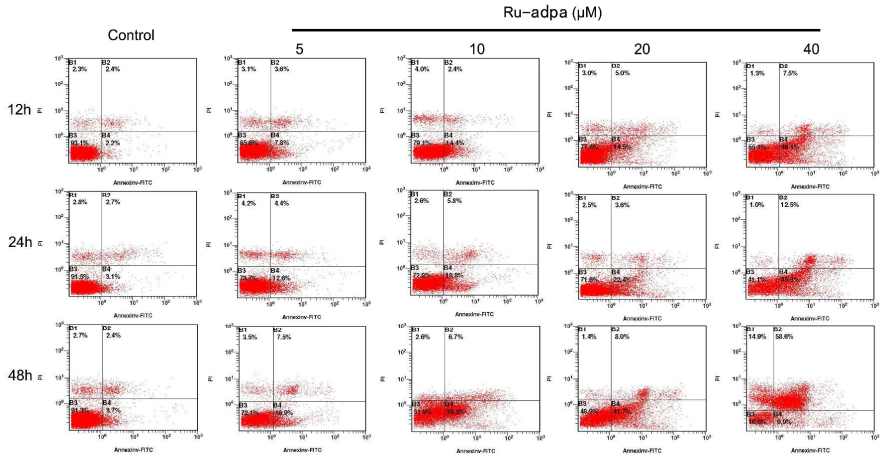

Fig.6 The percentage of living (B3), necrotic (B2), and apoptotic (B4) AGS cells

3.5 Cell cycle arrest

The distribution of AGS cells in various compartments during the cell cycle was analyzed by flow cytometry in cells stained with propidium iodide. As shown in Fig. 7, treatment of AGS cells with 5、10、20、40 μM **Ru-adpa** for 12 h cause significant enhancement of 3.1, 4.9, 10.8 and 19.7% in S phase compared with the control. On exposure of AGS cells to 5、10、20、40 μM **Ru-adpa** for 24 h, cause pronounced increases of 7.1, 11.2, 23.3 and 27.9% in S phase compared with the control. These data show that **Ru-adpa** induce S-phase arrest in AGS cells. (See Supporting Information Fig.S2)

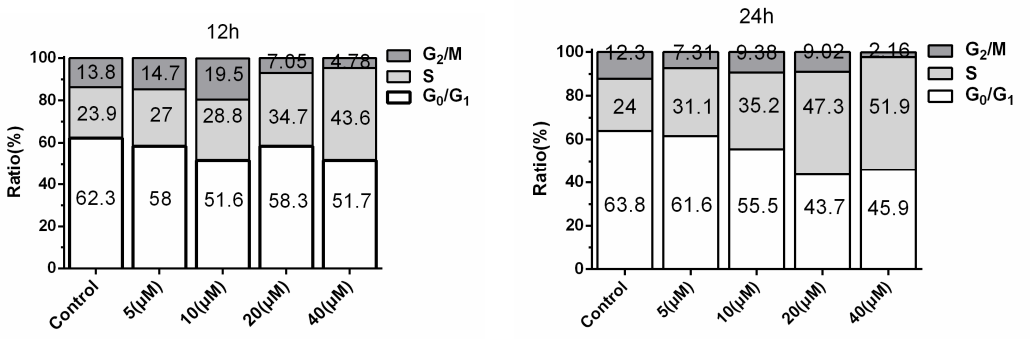

Fig.7 Cell cycle distribution on exposure of AGS cells to 5、10、20、40 μM **Ru-adpa**

3.6 Gel electrophoresis

Gel electrophoresis is a general method to evaluate the binding mode of small molecules and DNA base pairs.[38] In order to discuss how to interact the **Ru-adpa** with DNA, a gel electrophoresis study was performed on a 2000 bp length DNA segment from lpBR322(linear pBR322). We examined the effect of different concentration

ratios of the **Ru-adpa**, as the hexafluorophosphate, on DNA by monitoring the changes in the electrophoretic mobility of DNA in an agarose gel. The electrophoretogram of the DNA sample treated with different concentration ratios of the **Ru-adpa** is illustrated in Fig. 8. Lane 4 represents the gel moving pattern of pure DNA, as a control. Lanes 1-3 represent the DNA treated with the **Ru-adpa** in various concentration ratios. This electrophoretogram shows that the DNA samples in lanes 1-3 have moved slowly compared to the free DNA (lane 4) and that the migration of the DNA bands has been gradually retarded with the increase of the **Ru-adpa**. This observation clearly confirms that there is strong interaction between the **Ru-adpa** and DNA. Furthermore, the decrease in electrophoretic mobility of the bands demonstrates that the interaction of the **Ru-adpa** with DNA may occur via an intercalative mechanism, which could be facilitated further as a result of an electrostatic interaction between the **Ru-adpa** and the negative charges of the DNA. This observation could be explained on the basis that hydrophobic interaction of an intercalating ligand with DNA base pairs causes the double helix to become extended and locally uncoiled. Local unwinding of the double helix by an intercalating species results in an overall increase in the size of the DNA molecule.[39-40] This retardation behavior could also be attributed to the decrease of the overall charge of DNA due to binding with the **Ru-adpa**. Moreover, it was thought that intercalative interactions result in the band lag of the small molecule-DNA complex, while other binding modes do not affect the speed of band migration. We also ran the gel experiments for the effects of EB and H33258, EB is a classical intercalator of DNA and H33258 is a representative DNA-groove binder.[41] Obviously, EB made the band lag but H33258 did not affect the rate of the band. The results indicated that **Ru-adpa**, like EB, had obvious intercalative interactions with DNA.

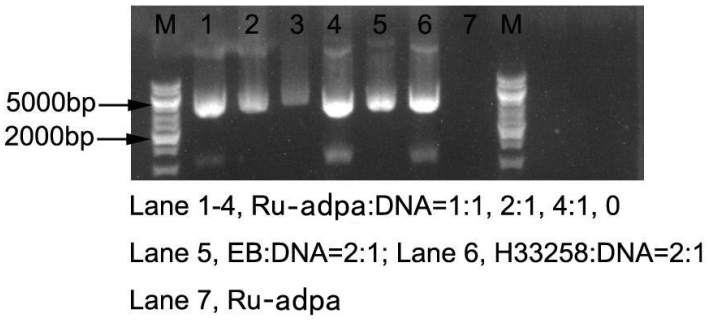

Fig.8 Gel electrophoresis of DNA in the presence of an increasing amount of **Ru-adpa** (Lane 1–4) and EB and H33258 acted as controls for classic intercalative interaction and groove interaction(Lane 5-6). M is the marker.

4. Conclusions

A novel ruthenium(Ⅱ) complex $[Ru(bpy)_2(adpa)](PF_6)_2$ was synthesized and characterized. In vitro, the **Ru-adpa** exhibits higher cytotoxicity toward AGS than BGC823 and SGC7901 cell lines under identical conditions. Hoechst 33258 staining and AO&EB staining demonstrated that **Ru-adpa** can effectively induce apoptosis of AGS cells. Apoptosis assay by flow cytometry showed the number of apoptotic cells increased with increasing concentration and time. The cell cycle arrest studies demonstrated that the antiproliferative effect induced by **Ru-adpa** on AGS cells occurs in S phase. In addition, the interactions between **Ru-adpa** and DNA were demonstrated to be intercalative binding.

Acknowledgements

This work was supported by the National Natural Science Foundation of China (No. 21101121), the Natural Science Fund (No. 2010CDB01301) of Hubei Province. the National Natural Science Foundation of China (No. 31170328 and 30900122), the Fundamental Research Funds for the Central Universities (No. 2014301020203).

References

[1] B. C. E. Makhubela, M. Meyer and G. S. Smith, *J. Organomet. Chem.,* 2014, **772**, 229.

[2] M. Alagesan, P. Sathyadevi, P. Krishnamoorthy, N. S. P. Bhuvanesh and N. Dharmaraj, *Dalton T.,* 2014, **43**, 15829.

[3] K.G. Lipponer, E, Vogel and B. K. Keppler, *Synthesis, Characterization and*

Solution Chemistry., 1996, **3**, 243.

[4] I. Berger, M. Hanif, A. A. Nazarov, C. G. Hartinger, R.O. John, M. L. Kuznetsov, M. Groessl, F. Schmitt, O. Zava, F. Biba, V. B. Arion, M. Galanski, M. A. Jakupec, L. Juillerat-Jeanneret, P. J. Dyson and B. K. Keppler, *Chem. Eur. J.,* 2008, **14**, 9046.

[5] C. G. Hartinger, M. A. Jakupeca, S. Zorbas-Seifrieda, M. Groessla, A. Eggera, W. Bergerd, H. Zorbasc, P. J. Dysonb and B. K. Keppler, *Chem & Biodivers.,*2008, **5**, 2140.

[6] O. Domotor, C. G. Hartinger, A. K. Bytzek, T. Kiss, B. K. Keppler and E. A. Enyedy, *J. Biol. Inorg. Chem.,* 2013, **18**, 9.

[7] M. Groessl, E. Reisner, C.G. Hartinger, R. Eichinger, O. Semenova, A. R. Timerbaev, M. A. Jakupec, V. B. Arion and B. K. Keppler, *J. Med. Chem.,* 2007**, 50***,* 2185.

[8] E. Reisner, V. B. Arion, B. K. Keppler and A. J. L. Pombeiro, *Inorg. Chim. Acta.,* 2008, **361**, 1569.

[9] L.Y. Ji, W. Zheng, Y. Lin, X. L. Wang, S. Lu, X. Hao, Q. Luo, X. C. Li, L. Yang and F.Y. Wang, *Eur. J. Med. Chem.,*2014,**77**,110.

[10] A. Srishailam, Y. P. Kumar, P. V. Reddy, N. Nambigari, U. Vuruputuri, S. S. Singh and S. Satyanarayana, *J. Photoch. Photobio. B.,* 2014, **132**, 111.

[11] F. A. Egbewande, L. E. H. Paul, B. Therrien and J. Furrer, *Eur. J. Inorg. Chem.,* 2014, **7**, 1174.

[12] P. Florindo, I. J. Marques, C. D. Nunes and A. C. Fernandes, *J. Organomet. Chem.,* 2014, **760**, 240.

[13] T. Joshi, V. Pierroz, C. Mari, L. Gemperle, S. Ferrari and G. Gasser, *Angew. Chem. Int. Ed.,* 2014, **53**, 2960.

[14] B. Peña, A. David, C. Pavani, M. S. Baptista, J.P. Pellois, C. Turro and K. R. Dunbar, *Organometallics.,* 2014, **33**, 1100.

[15] S. Grguric-Sipka, I. Ivanovic, G. Rakic, N. Todorovic, N. Gligorijevic, S. Radulovic, V. B. Arion, B. K. Keppler and Z. L. Tesi, *Eur. J. Med. Chem.,* 2010, **45**, 1051.

[16] J. Dubarle-Offner, C. M. Clavel, G. Gontard , P. J. Dyson and H. Amouri, *Chem.*

Eur. J., 2014, **20**, 5795.

[17] L. Messori, M. Camarri, T. Ferraro, C. Gabbiani and D. Franceschini, *Med. Chem. Lett.,* 2013, **4**, 329.

[18] C. S. Allardyce, P. J. Dyson, D. J. Ellis and S. L. Heath, *Chem. Commun.*, 2001, 1396.

[19] R. E. Morris, R. E. Aird, P. S. Murdoch, H. Chen, J. Cummings, N. D. Hughes, S. Parsons, A. Parkin, G. Boyd, D. I. Jodrell and P. J. Sadler, *J. Med. Chem.,* 2001, **44**, 3616.

[20] C.P Tan, S.S. Lai, S.H Wu, S. Hu, L. J. Zhou, Y. Chen, M.X. Wang, Y.P. Zhu, W. Lian, W.L .Peng, L.N. Ji and A.L. Xu, *J. Med. Chem.,* 2010, **53**, 7613.

[21] U. Schatzschneider, J. Niesel, I. Ott, R. Gust, H. Alborzinia and S. Wolfl, *ChemMedChem.,* 2008, **3**, 1104.

[22] S. Selvamurugan, P. Viswanathamurthi, A. Endo, T. Hashimoto and K. Natarajanc, *J. Coord. Chem.,* 2013, **66**, 4052.

[23] S. Sathiyaraj, K. Sampath, R. J. Butcher, R. Pallepogu and C. Jayabalakrishnan, *Eur. J. Med. Chem.,* 2013, **64**, 81.

[24] S. Sathiyaraj, R. J. Butcher and C. Jayabalakrishnan, *J. Mol. Struct.,* 2012,**1030**, 95.

[25] G. Raja, R. J. Butcher and C. Jayabalakrishnan, *Spectrochim. Acta. A.,* 2012, **94**, 210.

[26] A. Garza-Ortiz, P. U. Maheswari , M. Lutz, M.A. Siegler and J, Reedijk, *J. Biol. Inorg. Chem.,* 2014, **19**, 675.

[27] A. Garza-Ortiz, P. U. Maheswari, M. Siegler, A. L. Spek and J. Reedijk, *New. J. Chem.,* 2013, **37**, 3450.

[28] L. Hamryszak , H. Janeczek and E. Schab-Balcerzak, *J. Mol. Liq.,*2012,**165**,12.

[29] B. P. Sullivan, D. J. Salmon and T. J. Meyer, *Inorg. Chem.,*1978, **17**, 3334.

[30] I. Guezguez, A. Ayadi, K. Ordon, K. Iliopoulos, D. G. Branzea, A. M. Zalas, M. M. Janusik, A. E. Ghayoury and B. Sahraoui, *J. Phys. Chem. C.,* 2014, **118**, 7545.

[31] SMART and SAINT. Area Detector Control and Integration Software, Siemens Analytical X-Ray Systems, Inc., Madison, WI, USA, 1996.

[32] SHELXTL, version 5.0, Siemens Industrial Automation, Inc., Analytical Instrumentation, Madison, WI, 1995.

[33]T. Mosmann, *J. Immunol. Med.,* 1983, **65**, 55.

[34] G. J. Lin, G. B. Jiang, Y.Y. Xie , H. L. Huang, Z. H. Liang and Y. J. Liu, *J. Biol. Inorg. Chem.,* 2013, **18**, 873.

[35] B. Z. Pan, D.Q. Chen, J.Y. Huang, R. Wang, B. Feng, H. Z. Song and L.B. Chen, *Mol. Cancer.,* 2014, **13**,165.

[36] A. Riyasdeena, R. Senthilkumarb, V. S. Periasamyd, P. Preethya, S. Suresh, M. Zeeshanf, H. Krishnamurthy, S. Arunachalam and M. A. Akbarsha, *RSC Adv*., 2014, DOI: 10.1039/C4RA06702A.

[37] J.F. Li, R. Z. Huang, G. Y. Yao, M.Y. Ye, H.S. Wang, Y.M. Pan and J.T. Xiao, *Eur. J. Med. Chem.,* 2014, **86**, 175.

[38] Q.Y. Chen, D. H. Li, Y. Zhao, H. H. Yang, Q. Z. Zhu and J. G. Xu, *Analyst.*, 1999, **124**, 901.

[39] C. Deegan, M. McCann, M. Devereux, B. Coyle and D. A. Egan, *Cancer Lett.,* 2007, **247**, 224.

[40] A. D. Richards and A. Rodger, *Chem. Soc. Rev.,* 2007, **36**, 471.

[41] S. Y. Breusegem, R. M. Clegg and F. G. Loontiens, *J. Mol. Biol.,* 2002, **315**, 1049.